Excited state charge separation in symmetrical alkenes

Zijlstra, Robert Wiebo Johan

Excited State Dynamics of Tetraphenylethylene:

Ultrafast Stokes Shift, Isomerization and Charge Separation

5.1 Introduction

One of the most fundamental, yet simplest chemical processes involves rotation around a chemical bond. While many molecules exhibit this effect in the ground state, there are several important systems where isomerization is solely a photon driven process. The most famous example is rhodopsin[1], where a cis-trans isomerization in the retinal pigment triggers a series of events that ultimately lead to vision. The primary step in this reaction is thought to proceed via a nonadiabatic crossing to the ground state surface[2]. Other typical examples are molecules like stilbene and azobenzene. Stilbene is the prototype alkene and has been studied both in the gas[3] and condensed[4, 5] phases. Using a variety of nonlinear optical techniques, much has been learned about the initial dynamics along the reaction coordinate. Since cis-trans isomerization reactions occur on a picosecond time scale, this effect has potential for optical switching applications. When an alkene or azobenzene is embedded in a liquid crystal or polymer, photon induced isomerization leads to large structural changes in these materials[6, 7]. This effect could possibly be exploited for optical information storage. In the discussion of the photochemistry of stilbene the so-called "phantom state" plays a major role[8]. This is the lowest energy state along the twisting coordinate where the phenyl rings are (nearly) perpendicular to one another and which is presumed to be the activated complex for cis-trans isomerization. While in stilbene the energetic minimum occurs at a twist angle of ~105^0, in ethylene the perpendicular conformation has the lowest energy. Calculations show[9-11] that for ethylene an *avoided crossing* exists near the phantom state between the electronic states $^1B_2$ and $^1A_1$, which are the singly excited π-π^* and the doubly excited π^*-π^* states, respectively. Figure 5.1 shows a schematic picture of the energies of these states as a function of twist angle.

In the vicinity of the avoided crossing, where these states are degenerate within the Born-Oppenheimer approximation, the molecule becomes extremely polarizable. This effect is known as "sudden polarization"[12]. Small perturbations, as, for instance, induced by solvent collisions, heavily mix these levels, leading to states that exhibit large induced dipoles due to charge separation across the C-C bond. Such ionic states can be further stabilized by pyramidalization of one of the carbon centers, thus shifting the excited state charge distribution from a so-called biradical to a zwitterionic nature[9, 10].

Although solvent polarity has a marked effect on the lifetime of cis-stilbene[13], the importance of ionic states in the isomerization process has not been assessed yet. The same holds for rhodopsin and bacteriorhodopsin, although in the latter case an avoided crossing has been held responsible for the presence of a small barrier along the twisting coordinate[14].

In the case of ethylene it has been suggested[15] that the ion-pair character of the lowest excited state near the phantom configuration facilitates a 1,2 hydrogen atom shift in the photodecomposition process. For 9,9'-bianthryl (BA) and tetraphenylethylene (TPE), microwave conductivity[16, 17] and optical calorimetry[18, 19] measurements clearly showed twisting induced charge separation across the central C-C bond. This process is only possible when the intrinsic inversion symmetry of BA and TPE is broken by solute-solvent interactions. Since solvation-shell dynamics occur on time scales of 100 fs to

several ns, an intriguing question concerns the time scale on which symmetry breaking occurs.

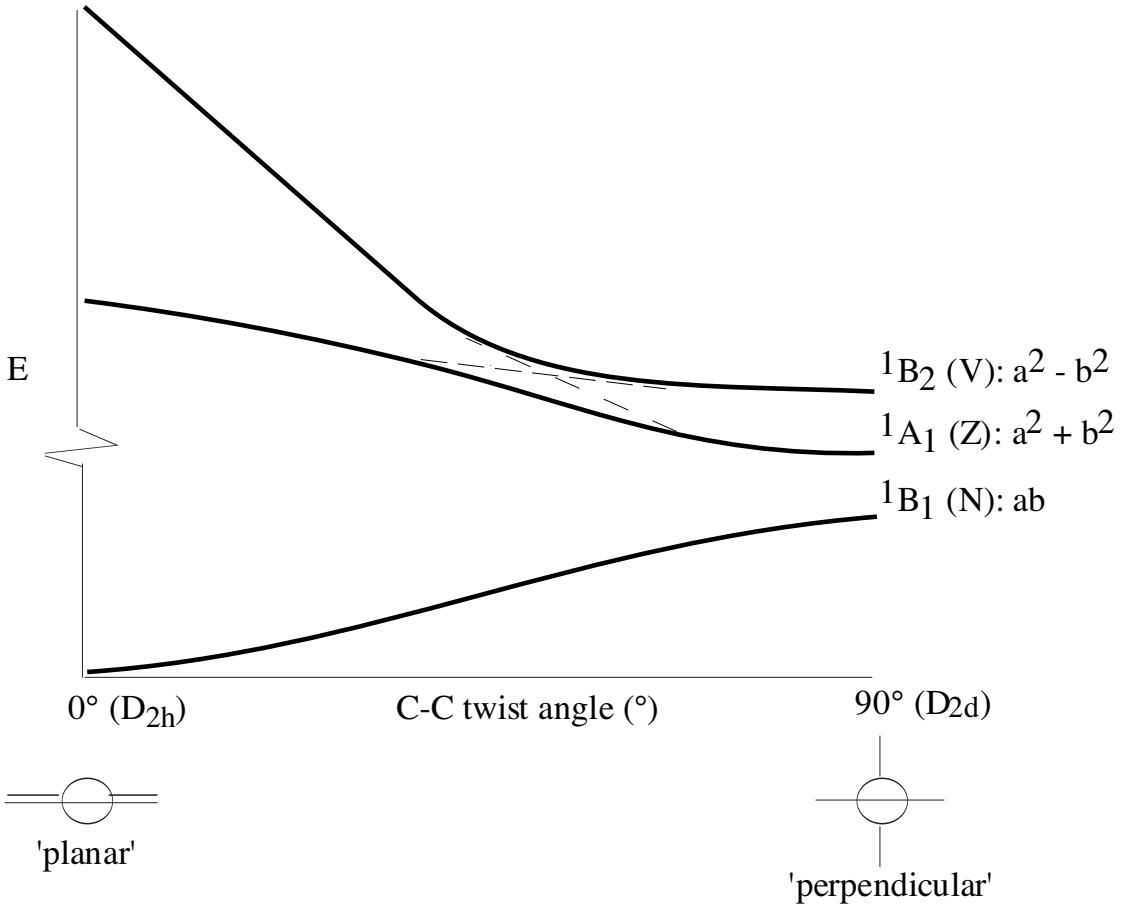

Figure 5.1 Schematic representation of the lowest potential energy surfaces of symmetric alkenes, as a function of the central bond twist angle. Newman projections of the two limiting cases of D_{2h} and D_{2d} symmetry are shown below. The position of the avoided crossing between the two excited states presumably depends on the substituents of the central alkene backbone. The nomenclature of the states (N, Z, V and ab, a^2+b^2, a^2-b^2) is explained in Section 5.4.

This chapter focusses on the twisting and charge-separation dynamics of TPE using femtosecond pump-probe spectroscopy. There is a long history on the spectroscopy and dynamics of TPE. Most noteworthy for TPE is its dual fluorescence and nonexponential fluorescence decay kinetics in nonpolar solvents. A landmark picosecond pump-probe study on TPE in 3-methylpentane was published in 1981 by Barbara *et al.*, who proposed a three-state model to account for the spectroscopy and dynamics around the central bond[20]. Although the nature of the intermediate states was not identified, the model accounted for all spectroscopic observations, including the large Stokes shift in emission, the dual fluorescence, the viscosity dependence of the fluorescence lifetime and the radiationless decay from the last state along the isomerization coordinate back to the ground state.

Soon thereafter Greene reported[21] that TPE in hexane has an excited state absorption at about 620 nm, which decays on a ps time scale. In view of earlier experiments on stilbene this time scale was attributed to twisting around the ethylenic bond. Greene also suggested a transient absorption at 420 nm to be due to a charge-resonance state, formed on twisting around the C-C bond. Schilling and Hilinski[22] examined the effect of solvent polarity on the decay of this band, and concluded from its solvation dynamics that a zwitterionic rather than a charge-resonance state was involved. They proposed that with increasing solvent polarity the zwitteronic state is stabilised, thereby reducing the energy gap with the ground state. This latter effect would also explain the increased rate for radiationless decay to the ground state in a polar solvent.

Morais *et al*. performed picosecond optical calorimetry measurements on TPE, which strongly suggested the existence of a zwitterionic state along the twist coordinate[18]. Ma *et al*. extended this study[19] and determined the energy differences between the two twisted states (the second and third state in the model of Barbara et al.) to be only a few kT. They went further and assigned the three states to the vertically excited state, the conformationally relaxed state and the twisted excited state, which they interpreted as a zwitterionic state.

Schuddeboom *et al*.[17] recently reported results of time-resolved microwave conductivity measurements on TPE in alkanes, which clearly showed the existence of a long-lived polar excited state. They further concluded that the so-called "prompt emission" of TPE, at about 500 nm, derives from a partially relaxed S_1 state, while the fluorescence around 560 nm was assigned to a conformationally relaxed S_1 state. They also suggested this latter state to be in equilibrium with the zwitterionic state.

Recently, Lenderink *et al*.[23, 24] reported the first results of a fs pump-probe study on TPE. On this time scale vibrational wave packet motion on the excited state potential and an ultrafast dynamic Stokes shift is observed. From the fact that the Stokes shift seemed to occur on the same time scale as the buildup of the wave packet motion, it was concluded that ethylenic bond twisting proceeds on a sub-ps time scale, just as in the case of cis-stilbene. The results presented in this chapter, however, are not in agreement with this earlier conclusion. In line with earlier work it is observed that ethylenic bond twisting in TPE takes place on a ps time scale and that the sub-ps Stokes shift dynamics is caused by ultrafast vibrational relaxation of the vertically excited state. The pump-probe data presented here further show that no phase shift occurs in the oscillatory transient probed at 650 run, as suggested earlier by Lenderink[23]. It turns out that these oscillations -which are much more pronounced in the measurements presented here- can be fitted very well assuming instantaneous response.

This chapter reports a detailed account of fs pump-probe measurements on TPE in solvents of different polarity, focusing in particular at the mechanism of the charge separation reaction. A novel finding is that in alcohols there is a direct relation between the decay of the 650 nm absorption and the buildup of the transient at 500 nm. In alkanes the latter signal exhibits a delayed buildup compared to the decay of the 650 nm band. In alcohols these dynamics relate the decay of the Franck-Condon relaxed planar excited state to the formation of a zwitterionic state. In alkanes this zwitterionic state is less stabilised and formed on a slower time scale. All these dynamics can be explained when the avoided crossing between singly and doubly excited states of TPE is taken into account. A unified description of the electron-transfer process is proposed in terms of

adiabatic crossing between solvation-dressed excited state energy surfaces. Large parts of the work described in this chapter have also been published in literature[25].

5.2 Pump-Probe Spectroscopy: A Short Introduction

The field of molecular dynamics has matured significantly by the development of spectroscopic techniques based upon non-linear optical phenomena[26]. Both intramolecular rearrangements as well as interactions with the environment on ground and excited state potentials can be studied in great detail using a wide variety of such techniques, aided by the continuing improvement of the resolution of such measurements. This is mainly due to the ongoing reduction of the temporal width of the laser pulses applied. It is beyond the scope of this thesis to give an extensive overview of the available techniques, nor is it the intention to provide the reader with a detailed theoretical description of pump-probe spectroscopy. Several excellent publications on the subject matter are available, and the interested reader is kindly requested to confer to these books and articles for more details[24, 26-28]. However, to be able to understand the processes under investigation when performing pump-probe spectroscopy, a general explanation of the technique will be given in this section.

Pump-probe spectroscopy is a time-resolved technique in which the evolution of a (non-equilibrium) system like an ensemble of molecules in a condensed phase is investigated. The experiment is initiated by applying an intense pump pulse to the system in order to drive it away from its equilibrium. This generally means that the system is brought into a (superposition of) photo-excited electronic state(s). Subsequently, these photo-excited states are probed by a second pulse, the probe pulse, which monitors the evolution of the system from its non-equilibrium starting point on the excited state potential energy surface(s). With the use of a short pump pulse, a system will generally be brought into a superposition of vibrationally excited states, which is commonly referred to as a vibrational wave packet[26]. This formalism is frequently used to describe the time-dependent evolution of a system under investigation.

$$\phi_j(q,t) = \sum_v c_{jv}(t)\phi_{jv}(q,t) = \sum_v c_{jv}(t)\phi_{jv}(q)\exp(-i\omega_{jv}t) \qquad \textbf{(5.1)}$$

In equation 5.1, ϕ_{jv} are the vibrational eigenstates of the nuclear Hamiltonian H_j of the time-dependent Schrödinger equation, with $\omega_{jv} = 2\pi E_{jv}/h$ as their energy eigenvalues. However, ϕ_j does not need to be an eigenfunction of H_j, in which case it can be written as the given sum of eigenfunctions ϕ_{jv} with coefficients c_{jv} and phase factors $-i\omega_{jv}t$. This is referred to as a vibrational wave packet.

In pump-probe spectroscopy, care has to be taken when probing with pulses with a broad spectral width, since the various parts of the frequency of the pulse can be temporally separated. Such frequency dependent time delay, usually referred to as a chirp[29], can lead to a destruction of the experiment when the first arriving frequencies effectively alter the state of the system, in which case the delayed frequencies probe a different state as intended. Another complication may arise when probing at the pump

wavelength, in which case coherent coupling effects may influence the excited state population. However, the experiments reported in this chapter are so-called dual colour pump-probe experiments, meaning that pump and probe pulses are located in non-overlapping frequency domains, thus avoiding the latter complication. In addition, the possible influence of a chirped pulse has been minimized by a number of measures, which are described in more detail in section 5.3.

A useful way to interpret the wave packet dynamics in pump-probe experiments is by means of the so-called 'doorway-window picture'[30]. In this approach, the dynamics of the system under investigation are assumed to take place at time scales which are significantly larger than the width of the pump-pulse, i.e. pump and probe pulse are well separated in time. This is an important precondition, since temporal overlap of these pulses gives rise to coherent interactions between the two, complicating the interpretation of the signals as a result. However, the pump pulse widths used in the here described experiments (vide infra) are in the 50-80 fs range, whereas the relevant dynamical processes take place in the (sub)picosecond domain, thereby generally obeying this precondition.

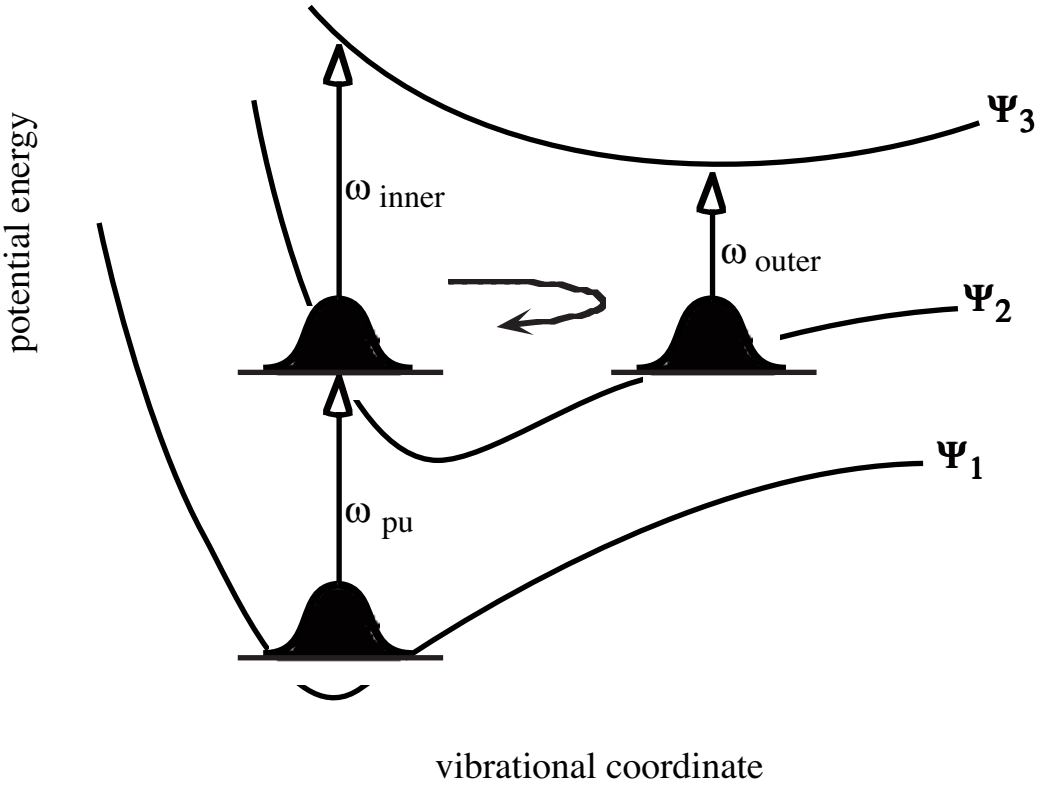

Figure 5.2 Schematic drawing of a pump-probe process in the doorway-window picture for a bound Ψ_2 potential. Upon excitation by a pump pulse with frequency ω_{pu}, the excited state wave packet moves back and forth between inner and outer turning points marked ω_{inner} and ω_{outer}, respectively.

In the doorway-window picture, a system is pushed into a non-equilibrium state through the doorway by the pump pulse, after which the probe pulse monitors the evolution of the wave packet 'from the outside' through a window (figure 5.2). A system is lifted from its ground state Ψ_1 to its excited state potential energy surface (PES) Ψ_2 by a

pump pulse with frequency ω_{pu}. In figure 5.2, Ψ_2 is chosen to be a bound potential, even though this is not necessarily the case. For example, photo-dissociation reactions take place on an unbound Ψ_2 (or another excited state PES). No further attention will be payed to such processes, since they bear no relevance to this work. On Ψ_2, the wave packet will periodically move back and forth between the inner and outer positions, which can be probed at frequencies ω_{inner} and ω_{outer}. If the resolution of pump and probe pulses is high enough, i.e about three times as short as the period of the wave packet oscillation, and $\omega_{inner} \neq \omega_{outer}$, the wave packet motion can be observed in the recorded transients. For instance, when probing at frequency ω_{outer}, the signal will be low at t=0 due to the fact that the wave packet is mainly located at the inner side of Ψ_2. However, when probing with the same frequency half a period later, the intensity of the transient will have reached a maximum because the wave packet will have moved to the outer side of the PES. This way, intramolecular vibrational modes can be observed, which can provide valuable insights in the ultrafast processes of systems under investigation. Although not depicted in figure 5.2, probing can also induce a transition from Ψ_2 back to Ψ_1 (i.e. stimulated emission).

When using linearly polarized pulses, the pump pulse will create a polarization anisotropy in the system. Molecules having the relevant transition dipole oriented in parallel with the polarization direction of the pump pulse have a larger chance of being excited to Ψ_2 than molecules in which this orientation is of a perpendicular nature. This can be quantified in the following manner[31]. Assume a molecular axis system that coincides with the principle axis of the diffusion tensor. Its orientation with respect to the laboratorium fixed axis system can be defined in terms of the three Euler angles $(\alpha, \beta, \gamma) = \mathbf{\Omega}$. A normalized probability distribution can be defined as $f^{(i)}(\mathbf{\Omega}, t)d\mathbf{\Omega}$, describing the probability of finding a molecule in level (i) with an orientation between $\mathbf{\Omega}$ and $d\mathbf{\Omega}$. Now, the number density of molecules in electronic state i is given by:

$$K^{(i)}(t) = \int d\mathbf{\Omega} f^{(i)}(\mathbf{\Omega}, t) \qquad \textbf{(5.2)}$$

with integration limits according to the conventional limits of Euler angles.

In order to allow quantification of f(i), orientation-dependent operators are defined that enable the definition of the effective parallel and perpendicular concentrations of molecules giving rise to electric-dipole emissions or absorptions from a given level:

$$\begin{aligned} N_{\parallel}^{(i)}(t,\gamma) &= d\mathbf{\Omega}\hat{P}_{\parallel}(\mathbf{\Omega}, \gamma) f^{(i)}(\mathbf{\Omega}, t) \\ N_{\perp}^{(i)}(t,\gamma) &= d\mathbf{\Omega}\hat{P}_{\perp}(\mathbf{\Omega}, \gamma) f^{(i)}(\mathbf{\Omega}, t) \end{aligned} \qquad \textbf{(5.3)}$$

In equation 5.3, $\hat{P}_{\parallel}(\mathbf{\Omega}, \gamma)$ and $\hat{P}_{\perp}(\mathbf{\Omega}, \gamma)$ are proportional to the probabilities of a molecule with orientation $\mathbf{\Omega}$ having a transition dipole with a direction cosines in the molecular axis system γ, interacting with a light field polarized in the laboratory z (parallel) or laboratory x or y (perpendicular) directions, respectively. The operators are normalized such, that:

$$K^{(i)}(t) = N_{\parallel}^{(i)}(t, \gamma) + 2N_{\perp}^{(i)}(t, \gamma) \qquad \textbf{(5.4)}$$

regardless of orientation γ. An effective anisotropy associated with transition dipole γ can be defined as follows:

$$r^{(i)}(t, \gamma) = \frac{N_{\parallel}^{(i)}(t, \gamma) - N_{\perp}^{(i)}(t, \gamma)}{N_{\parallel}^{(i)}(t, \gamma) + 2N_{\perp}^{(i)}(t, \gamma)} \qquad \textbf{(5.5)}$$

where the following relations hold:

$$N_{\parallel}^{(i)}(t, \gamma) = \frac{1}{3}K^{(i)}(t)[1 + 2r^{(i)}(t, \gamma)]$$
$$N_{\perp}^{(i)}(t, \gamma) = \frac{1}{3}K^{(i)}(t)[1 - r^{(i)}(t, \gamma)] \qquad \textbf{(5.6)}$$

$r^{(i)}(t, \gamma)$ contains information about the orientational distribution of the transition dipoles γ for molecules in state (i). Description of an experiment is now reduced to defining appropriate expressions for the time-dependent r and K functions. In the experiments described in this chapter, only one initial state is mainly prepared, and r(t) is given by the familiar expression (equation 5.7) involving the second Legendre polynomial (P_2) of the correlation of the transition-moment direction at t = 0 with that at at time t.

$$r(t, \gamma) = \left\langle \frac{2}{5} P_2(\mu(0) \bullet \gamma(t)) \right\rangle \qquad \textbf{(5.7)}$$

For example, at $t = t_0$ combining (5.5) and (5.7) leads to an initial ratio around 3:1 for parallel and perpendicularly oriented populations when the pump and probe transition dipoles are oriented in a (near-)parallel fashion.

When using polarized pulses, an experiment may be performed at the 'magic angle', a fixed angle (54.7˚) between the respective fields of polarization of the linearly polarized pump and probe pulses at which depolarization effects, as for instance caused by molecular reorientation in the solvent, are averaged out. This allows straightforward interpretation of the data, which is especially useful if one is particularly interested in the intramolecular dynamics rather than, for instance, the behaviour of the molecule in its solvent cage. However, as will be demonstrated in this and the following chapter, the nature and driving forces of inter- as well as intramolecular dynamics can become apparent by performing polarization dependent measurements at various angles and comparing their outcome. Therefore, all experiments reported in these chapters were performed at parallel and perpendicular orientation of the pump and probe pulse polarization direction to obtain a qualitative impression of the depolarization processes in TPE.

5.3 Experimental

The femtosecond pump-probe experiments were performed with an amplified CPM-laser system[23, 24], yielding 10 μJ pulses at 620 nm with a repetition rate of 9 kHz. The pump pulse at 310 nm was generated by frequency doubling in a 300 μm thick KDP crystal, while probe pulses were derived from a continuum, obtained by focusing part of the amplified pulse in a 2 mm thick sapphire plate. The chirp in the continuum was removed by use of a pair of quartz prisms in nearly retroreflecting geometry and a double-pass grating pair, resulting in cross-correlation widths between pump and probe of 70-100 fs in the frequency range of 450-700 nm. This corresponds to continuum pulse widths of 50-65 fs for these parts of the spectrum.

The pump-probe signals were measured for parallel and perpendicular polarizations of the pump and probe pulses. Frequency selection was achieved by placing suitable interference filters in front of the photodiode detector. In addition, the spectrum of the continuum was narrowed in front of the sample, by positioning an adjustable slit in the probe beam after the first passage of the two quartz prisms. In this way, only the desired part of the total spectrum, with a width of about 50 nm, reaches the sample. This proved to be essential, since otherwise probe pulse-induced artefacts determine the observed transients.

Previously, Lenderink[23] used the uncompressed continuum as a probe with frequency selection behind the sample. A consequence of this arrangement is that all frequency components of the continuum interact with the sample. Although the probe pulse may be weak for a given spectral component, the pulse energy, integrated over the entire spectrum, is sometimes capable of altering the state of the system. In particular for experiments on the blue side of the spectrum, where light arrives with a time delay for a positively chirped pulse, a totally different state may be probed than originally excited by the pump pulse. To some extent, this proved indeed to be the case, since the transients reported by Lenderink differ occasionally from those shown here. The lesson learnt is that it is much preferred to perform wavelength selection in front instead of behind the sample.

Tetraphenylethylene (TPE) was recrystallized from ethanol/chloroform mixtures until whiteness was obtained. Following crystallization, the purity of TPE was checked by ^{13}C NMR and determination of the melting point (226-227° C, uncorrected). Cyclohexane, ethanol and 1-butanol (Merck, p.a.) and 1-octanol (Aldrich) were used as received. The investigated solutions were >99% pure, based on GC analysis. The sample consisted of a 300 μm free flowing jet with 0.2 mM 300 ml solutions. In cyclohexane solutions, the TPE concentration may have been slightly higher, due to the volatility of cyclohexane. This effect was compensated for by slowly adding cyclohexane to the solution. GC analysis of the solutions after the experiment showed no evidence of buildup of photobyproducts.

5.4 Nomenclature of the States near the Avoided Crossing

Before the results of the experiments are discussed, the character of the states involved in the "sudden polarization" phenomenon will be commented upon. The parent molecule C_2H_4 will serve as an example. Around the 90^0 twisted conformation, one deals

with a two-electron, two-orbital open shell problem[32]. Indicating the p-orbitals on the two carbon atoms that form the double bond in the ground state, as "a " and "b", the states $^1(ab)$, $^1(a^2\pm b^2)$, and $^3(ab)$ arise, of which only the last one can be described - as far as the energy is concerned - with a single determinant wave function. States with a dipole moment, in which the electron density on one of the carbon atoms is higher than that on the other carbon atom, are associated only with the $^1(a^2\pm b^2)$ states. At the twist angle where the $^1(a^2+b^2)$ and $^1(a^2-b^2)$ Born-Oppenheimer surfaces cross (see Fig. 1), these two states are degenerate and any appropriate symmetry lowering interaction, be it intramolecular (Jahn-Teller effect) or external (solvent reorganization), will induce localization of the electronic charge distribution on one side of the molecule. This leads to an avoided crossing and to solvent stabilization of a charge-transfer state $^1(c_1a^2+c_2b^2)$, where $c_1 \gg c_2$ or vice versa. This is also known as a "zwitterionic-", or, referring to the D_{2d} parent state, as the "Z"-state.

Thus, the $^1(a^2+b^2)$ state is "stabilized" by symmetry breaking, which leads to a new state with an appreciable dipole moment. In contrast, the $^1(a^2-b^2)$ state, also known as the "V" state, is destabilized by solvation. Hence, there is a tendency to reduce the dipole moment when the molecule is on this potential surface. The $^1(a^2-b^2)$ state itself carries no dipole moment, which has led -erroneously- to classifying it as a "biradical" state. Note that the V and Z states are no longer orthogonal, when dressed with the solvent-interactions as described here.

In the practice of organic chemistry and ESR spectroscopy, it is common to use the phrase "biradical" for systems where two unpaired electrons are localized on relatively distant parts of the molecule and consequently the singlet/triplet splitting is small. For C_2H_4 and the like, the only states that may give rise to this situation are the $^{1,3}(ab)$ states. The CT states are essentially singlets and cannot be "biradical" at all. We will therefore call a state "charge resonance" (CR) when the electron distribution is symmetric, and "charge transfer" (CT) or "zwitterionic" when an electron has been transferred from one half of the molecule to the other.

In light of the above discussion, the assignment of a transient absorption at 1000 nm in the ethylenic system biphenanthrenylidene to a biradical-zwitterionic transition, by Piotrowiak *et al* [33] is, most likely, incorrect. The lack of a solvatochromic effect on this transition strongly suggests the initial and/or final states to have only a very weak CT character, indicative of a small interaction between the two non-degenerate energy surfaces.

5.5 Results and Discussion

5.5.1 The First Two Picoseconds

The initial pump-probe response of TPE, up to about two picoseconds, is solvent independent. This suggests that on this time scale the dynamics are predominantly intramolecular. Figure 5.3 displays typical transients for TPE in cyclohexane at probe wavelengths from 500 to 650 nm. At all wavelengths, from 450 to 700 nm, the absorption rises instantaneously, which is interpreted as a signature of excited state absorption. While

the green part of the spectrum displays fast changes, the transient absorptions at 450 nm and in the 600-650 nm range persist on a ps time scale, as already noted by Greene[21].

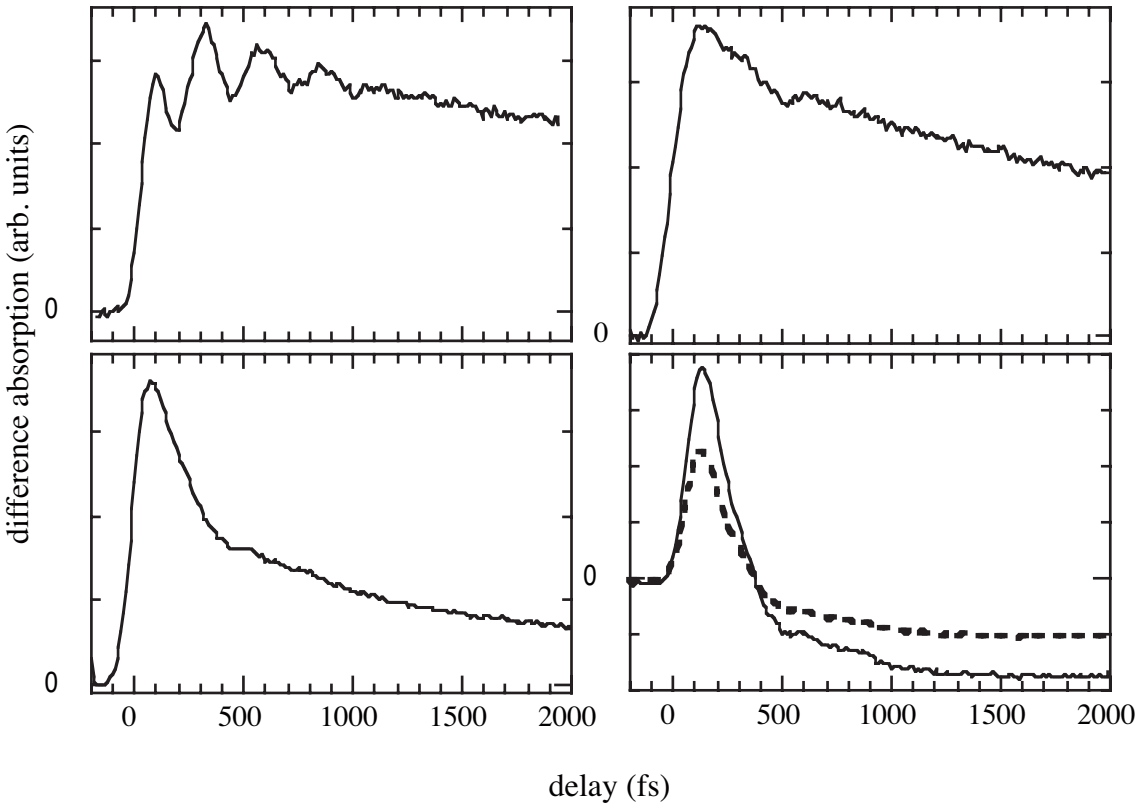

Figure 5.3 Pump-probe spectra of TPE in cyclohexane up to 2 ps. In all cases the excitation wavelength is 310 nm. The probe wavelengths are 650, 600 (top left and right panels), 550 and 500 nm (bottom left and right panels). All transients are largely solvent independent. For λ_{pr}=500 nm, the results for both parallel (solid line) and perpendicular (dashed line) pump and probe polarization are shown.

As shown in the bottom right panel of figure 5.3, the transient at 500 nm changes sign after a few hundred femtoseconds. The excited state absorption turns into a bleach, which is assigned to stimulated emission. This signal is largest for parallel pump and probe polarizations. In TPE, the $S_1 \leftarrow S_0$ transition is polarized along the p_z orbitals, which form the central double bond. The fact that the stimulated emission remains polarized along the excitation direction over the first 2 picoseconds, implies that on this time scale no ethylenic bond twisting occurs. The transient stimulated emission, probed at 500 nm, therefore must reflect vibrational cooling from an initial state that has kept its ground state configuration, except for elongation of the central C-C bond. Indeed, the C-C bond in the π-π^* excited state is formally a single bond, which is stretched compared to the ground state. This picture is corroborated by the resonance Raman spectrum of TPE, which is dominated by the 1585 cm^{-1} stretching vibration of the central bond[24]. The vertically excited state therefore quickly relaxes to the potential minimum along the C-C stretch mode, by coupling to other intramolecular vibrations. Thereby, a sizable Stokes shift is generated.

The Stokes shift of 12,000 cm^{-1}, observed in the stimulated emission, is indeed large. Although this suggests a large structural change in the TPE excited state[23], calculations on the parent molecule ethylene confirm that a lengthening of the C-C bond in the excited state of about 0.3 Å accounts for a shift of 11,000 cm^{-1}. This ab initio calculation was performed at the all-valence CISD level in a standard double zeta valence (DZV) basis for the planar geometry (C-H bond length 1.076 Å; H-C-H bond angle 116.6^0). The fact that the Stokes shift occurs on a subpicosecond time scale and is solvent independent, points to strong intramolecular vibrational coupling, leading to fast energy redistribution among the many modes of TPE.

At 650 nm, the pump-probe signal exhibits strong oscillations due to a low frequency vibration (124 cm^{-1}), which decays on a subpicosecond time scale. Previously, Lenderink[23] assigned this mode to a torsional and/or scissoring motion of the phenyl rings. The oscillations displayed here are much more pronounced than reported earlier, which is probably due to the fact that in the previous experiments the probe pulse carried a substantial chirp. This may enhance or suppress the wave packet dynamics, depending on the sign of the chirp[29, 34]. The first impression from the trace at 650 nm (see the top left panel of fig. 5.3) is that the wave packet builds up in time. Previously, this was interpreted as a phase shift[23], caused by indirect excitation of this mode by, for instance, the C-C strech mode. However, closer inspection of these transients obtained with higher time resolution, reveals that the apparent build-up results from the finite pulse durations used in the pump-probe experiment. Figure 5.4 shows that an excellent fit to the pump-probe data at 650 nm can be obtained by convoluting the experimental time resolution with a response function of the form[5]:

$$M(t) = A_{650} \exp(-t/\tau_{650}) + B_{osc} \exp(-t/\tau_{osc}) \times \cos[2\pi\nu_{osc} + \theta] \qquad \textbf{(5.8)}$$

with phase $\theta=0$. Here, A_{650} and τ_{650} are the amplitude and decay time of the overall response at 650 nm, while B_{osc} and τ_{osc} are the same quantities for the vibrational wavepacket with frequency ν_{osc}. Fits with a quality similar to that of figure 5.4 could be obtained for all solvents, with phase $\theta=0$. This indicates that the wave packets are directly excited from the ground state. The fit parameters are shown in Table I. Damping of the torsional mode increases slightly at higher solvent viscosity, showing the importance of intermolecular vibrational mode coupling for these low frequency, large amplitude motions.

For a probe wavelength of 700 nm, the same 124 cm^{-1} motion of the phenyl rings dominates the response. Surprisingly, again a phase shift $\theta=0$ is found (see also figure 5.2 for a graphical representation of the involved process). The presence of a steep higher-excited state potential in the probing process may be the explanation for this probe wave length independent phase. This interpretation implies that shifts should be observable much further to the red of the current probe wave lengths. At the moment, it has not been possible to probe in that range yet.

solvent	lifetime τ_{650} (ps)	frequency ν_{osc} (cm^{-1})	damping τ_{osc} (fs)
ethanol	4.2	122	305
1-butanol	6.7	124	345
1-octanol	9.9	123	430
cyclohexane	11.8	126	406

Table 5.1 Parameters of the fits of the wave packet motion at 650 nm. The overall damping of the pump-probe transient at this wavelength (τ_{650}), the frequency of the oscillation (ν_{osc}) and the damping time of the oscillation (τ_{osc}) are listed for the various solvents.

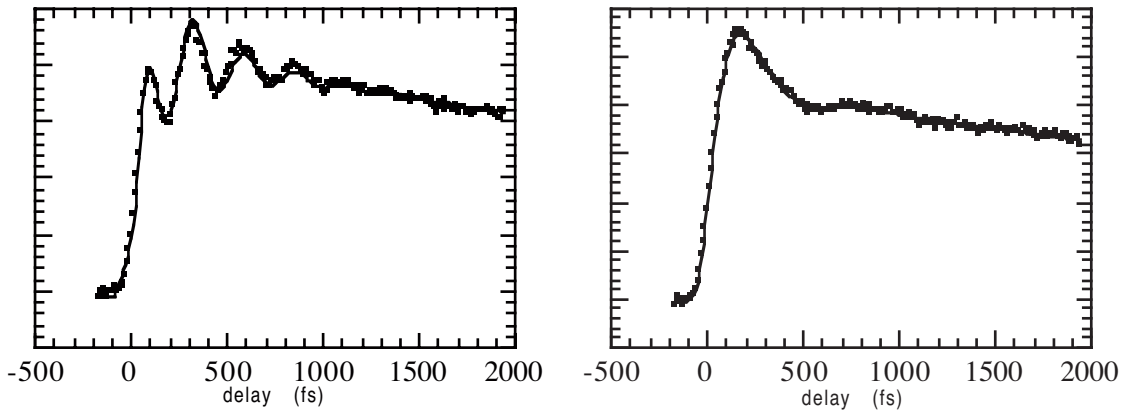

Figure 5.4 Fits (solid lines) to the two type of oscillations, observed in the short-time pump-probe spectra of TPE (dots). In the left panel the result is shown for the 650 nm transient of TPE in cyclohexane; in the right panel that for the 600 nm transient of TPE in octanol. The parameters of the fits at 650 nm can be found in Table I for the different solvents. The parameters for the fits of the much weaker oscillation at 600 nm were, within the experimental error margins, identical for all solvents.

At the high energy side (500-600 nm) the transients do not display this phenyl ring motion, but instead a slight undulation at lower frequency is observed. As shown in figure 5.4 for the 600 nm transient of TPE in octanol, this can be fitted with equation 1 as well, yielding a mode of about 58 cm^{-1}. This frequency is close to one observed in pump-probe spectra of rhodopsin. There, a 60 cm^{-1} mode is assigned to a skeletal torsional mode, associated with the isomerization reaction coordinate[2].

5.5.2 Longer Time Scales

Figure 5.5 displays the pump-probe transients for TPE in cyclohexane and ethanol on longer time scales. All transients show a pronounced solvent dependence, which relates to twisting around and charge separation across the central carbon-carbon bond. The time scale of the twisting motion is most apparent in the decay of the excited state absorption at

650 nm. In this spectral region the signals do not depend very much on the relative orientation of the pump and probe polarizations, but a marked dependence on solvent viscosity is observed. Note that in cyclohexane after about 15 ps a plateau is reached.

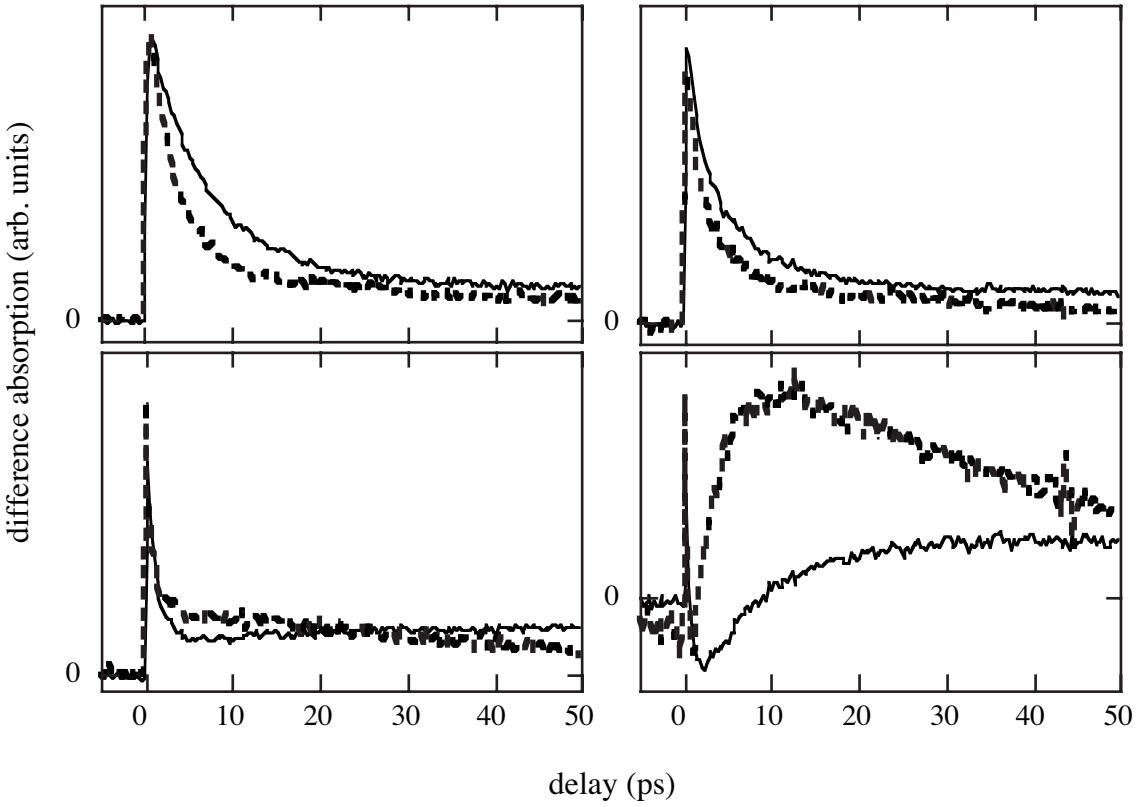

Figure 5.5 Comparison between the ps pump-probe transients of TPE in cyclohexane (solid line) and ethanol (dashed line). The probe wavelengths are 500, 550 (bottom right and left panel), 600 and 650 nm (top right and left panel). For all alcohols, the decay in the red part of the spectrum is related to the rise of the signal in the green. For cyclohexane, no such relation is found.

In alcohols the 650 nm transient shows a faster decay, reaching a plateau within 10 ps. On a longer time scale this "plateau" decays with a lifetime which strongly depends on solvent polarity. Evidently, phenyl twisting in TPE proceeds on a time scale of several picoseconds instead of a few hundred femtoseconds as originally concluded[23]. This is about the same time scale as observed for trans-stilbene but a factor of ten slower than for cis-stilbene. Replacement of an ethylenic hydrogen atom in stilbene by a phenyl ring in TPE decreases the electron pair repulsion due to some delocalization, while increasing the solvent drag. The isomerization rate in any of these alkenes is determined by a subtle balance between electrostatic and steric factors, making it difficult to compare these molecules.

The most dramatic solvent dependence on the ps transients is observed in the 500-550 nm region. In this spectral region the transients are not only sensitive to solvent viscosity but also to solvent polarity. Figure 5.6 displays these transients for three different alcohols and cyclohexane. This figure clearly shows that the ps transients for ethanol and cyclohexane are very different, even though their viscosities are similar. For

the longer alcohols the buildup and decay become progressively slower, by the increase of viscosity and the decrease of polarity. We further note that for alcohols a direct relation is found for the decay of the 650 mn band and the buildup time of the 500 nm absorption, that follows after the stimulated emission signal at this wavelength (figures 5.5 and 5.6).

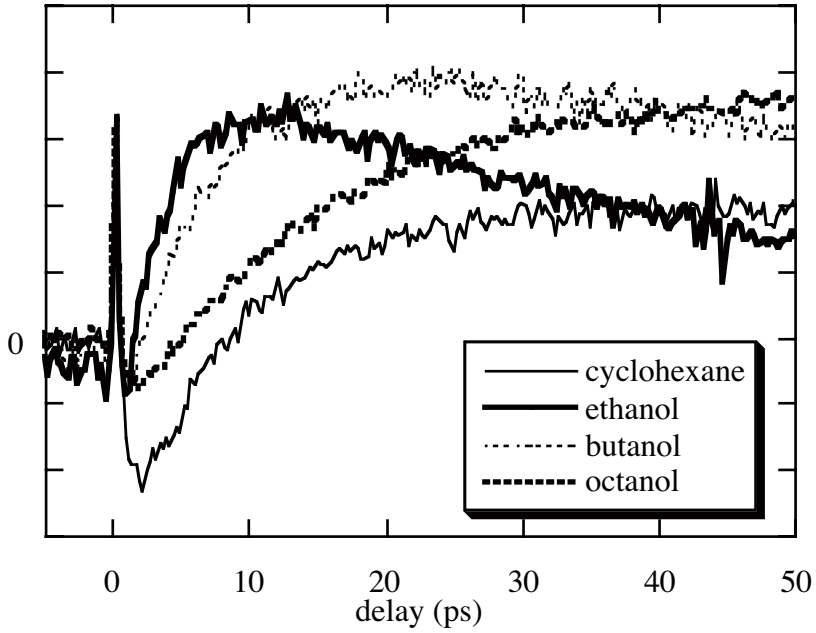

Figure 5.6 The picosecond dynamics of TPE at 500 nm in ethanol, 1-butanol, 1-octanol and cyclohexane. In this part of the spectrum, the pump-probe transients are strongly dependent on the polarity and the viscosity of the liquid, as discussed in the text.

These observations suggest that the 500 nm transient is connected to a species, directly generated from the Franck-Condon relaxed excited state. Because of the strong polarity dependence of the rise and decay of the 500 nm transient, which is strongest for perpendicular polarizations, this species is suggested to be the zwitterionic state of TPE. Apparently, the Franck-Condon relaxed excited state is converted into a zwitterionic state by motion along the twist coordinate.

In order to characterize the dynamics, a simple kinetic analysis of all transients observed at the various wavelengths was performed. In this way the various time scales of the overall dynamics are determined, which facilitates the construction of the quantum mechanical picture presented in the next section.

It was found that a two-state model excellently fits the ps excited state dynamics of TPE in alcohols, and most likely in all polar solvents. A satisfactory fit to each set of transients was obtained, using a global fitting routine. Herein, all transients for a given alcohol are fitted simultaneously, with the same rate constants but different spectral amplitudes. In this fitting procedure the 500, 550, 600 and 650 nm transients have been included using a simple two-state consecutive reaction scheme. Figure 5.7 displays the resulting fits for ethanol; the quality of the fits for butanol and *n*-octanol is equally good. A careful look at the 550nm transient reveals a small discrepancy between the data and the fit at a delay of about 4 ps. As will be discussed below for the case of TPE in cyclohexane,

this small discrepancy is indicative of the presence of a third state in the dynamics. However, since in polar solvents this state apparently is hardly populated, the two-state model provides an adequate fit to the data.

For cyclohexane, the decay of the 650 nm transient is not directly related to the buildup of the 500 nm transient. Consequently, the results can not be fitted within a two-state model, as shown in figure 5.8. However, a three-state model, in which a dynamic equilibrium exists between two product states, works well. The reaction scheme covering the dynamics in both polar and nonpolar solvents therefore is the following:

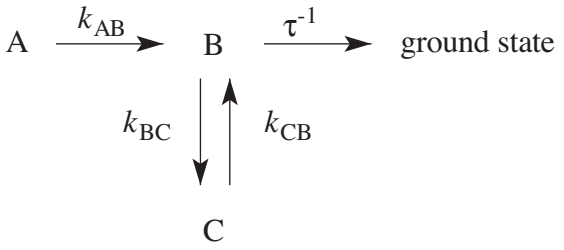

(5.9)

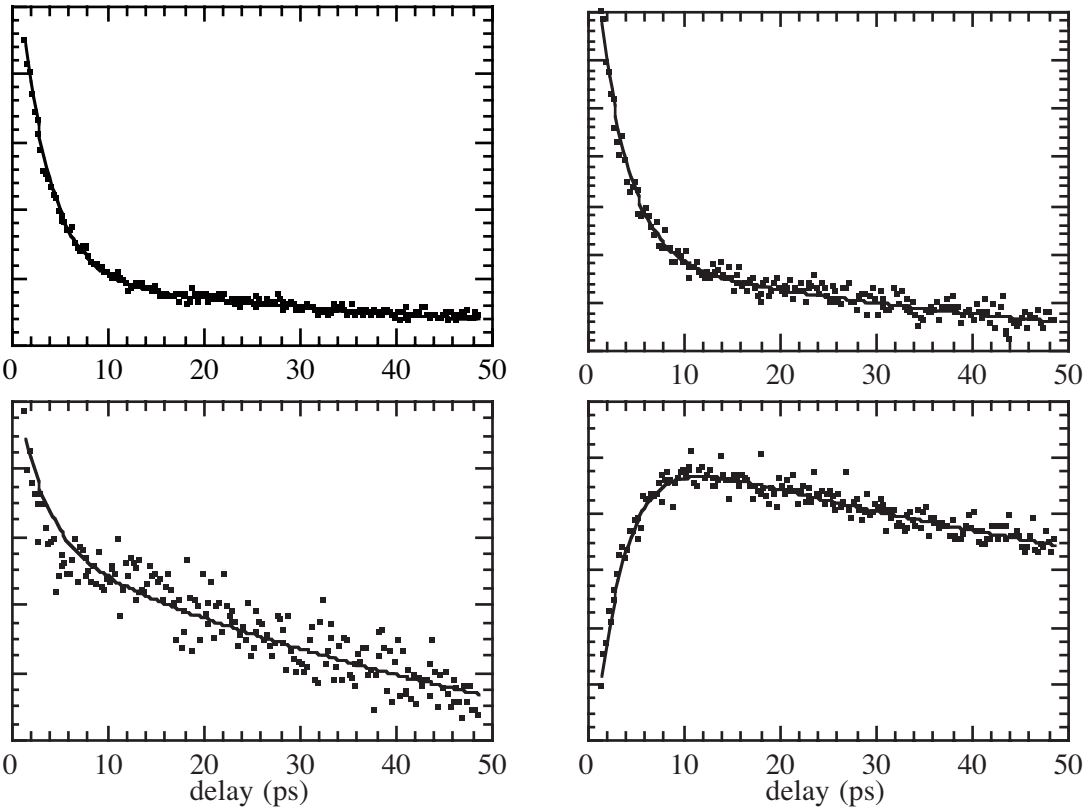

Figure 5.7 Fits (solid lines) of the 500, 550 (bottom right and left panels), 600 and 650 (top right and left panels) nm transients of TPE in ethanol (dots). For simplicity, the solvent independent ultrafast part of the response (<2 ps) was excluded from the fitting. A two-state model suffices to explain the data at all wavelengths with the same set of dynamic parameters. These are given in Table 5.2.

Excellent fits for the transients at all wavelengths are obtained for TPE in alcohols and cyclohexane as well, when the equilibrium with the third level is taken into account. In

principle, there could also be some direct transfer from A to C, involving k_{AC} as yet another kinetic parameter. The present data are not accurate enough to either exclude or identify this reaction path.

All parameters obtained from fitting the pump-probe transients to the two- and three-state models are given in Table 5.2. For the alcohols no values can be given for the kinetic parameters of the equilibrium between B and C, since C is not, or hardly, populated ($k_{BC} \ll k_{CB}$). These data show that the reaction rate out of state A is strongly influenced by the viscosity of the solvent, while state B has a lifetime that is directly related to the solvent polarity.

At this point it is noted that an interpretation of the transients, just discussed, in terms of vibrational relaxation phenomena is ruled out. Although the time scale for the observed effects is right, the excellent correspondence between the rise and fall times of these transients at different wavelengths in alcoholic solutions, but not for cyclohexane, is a very strong point for the interpretation given. Of course, effects of vibrational cooling should be present, for instance, in the spectral width of the transients involved. This is outside the scope of the present study.

When these results are considered in the light of the qualitative discussion presented above, the identification of states A, B and C seems clear. State A is suggested to be the vibrationally relaxed planar S_1 state, which is formed on a subpicosecond time scale from the vertically excited state. This state predominantly absorbs in the red part of the spectrum, while at 500 nm stimulated emission to the ground state occurs.

solvent	k_{AB} (ps^{-1})	k_{BC} (ps^{-1})	k_{CB} (ps^{-1})	τ (ps)
ethanol	0.32			60
1-butanol	0.15			350
1-octanol	0.07			$\sim 10^3$
cyclohexane	0.46	0.042	0.082	$>>10^3$

Table 5.2 Kinetic parameters for the dynamics of excited state TPE. A is the Franck-Condon relaxed planar configuration, B the zwitterionic (dipolar) state, and C is the charge resonance twisted state with an approximately symmetric charge distribution across the C-C bond. The k's are the rate constants for the transitions, and τ is the lifetime of the excited state.

This planar configuration subsequently decays on a ps time scale through a twist around the central C-C bond, accompanied by charge separation across this bond. Hence, B is the zwitterionic form of TPE, which has distinct polar character. Its main spectral feature is the strong absorption at 500 nm. This state subsequently decays to a twisted conformation on the ground state potential surface, or establishes an equilibrium with state C, the charge-resonance form of perpendicular geometry, which weakly absorbes over a large frequency range.

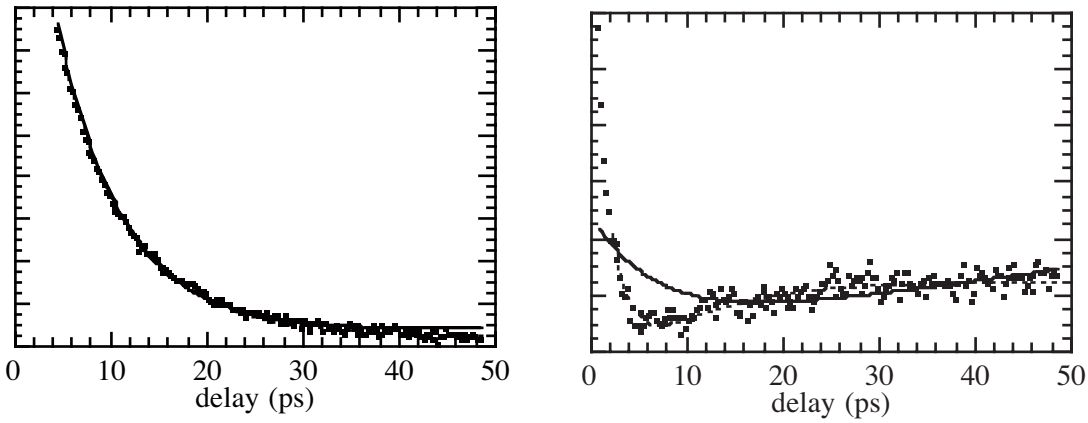

Figure 5.8 Fits of the 650 nm (left panel) and 550 nm (right panel) transients of TPE in cyclohexane. The fits to the data (dots) of the two-state model (solid lines) are clearly not as good as those of the three-state model (dashed lines). In nonpolar solvents, the transients at all wavelengths can only be simulated consistently, with the same dynamic parameters, when (at least) three states are involved in the dynamics. The parameters of the fits are given in Table 5.2.

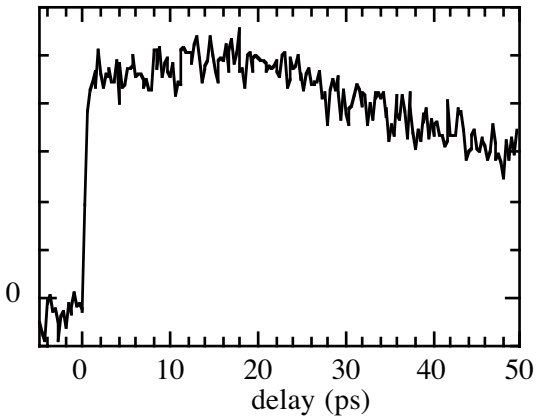

Figure 5.9 The picosecond dynamics of TPE in ethanol for probing at 450 nm. Apart from a small rise, due to the wing of the 500 nm band, only the overall decay of the excited state population is observed. Twisting and charge separation do not significantly influence this part of the spectrum.

In cyclohexane, both the charge-resonance state and the zwitterionic form are populated appreciably. In alcohols, the equilibrium is strongly shifted towards the zwitterionic state; in fact the charge-resonance form in these solvents is hardly detected at all. The small discrepancy in the two-state fit of the 550 nm transient of figure 5.8 is due to the very limited and short-lived population of this state. The stabilization of the zwitterionic state in polar solvents is caused by the interaction between the induced dipole of the zwitterion and the dipoles of the solvent. As a result, the charge-resonance state is largely bypassed and/or its lifetime in polar solvents is so short that its transient

population can hardly be detected at all. This analysis is supported by the observation of a broader transient spectrum in the 500-550 nm range in cyclohexane compared to alcohols, which suggest that the red flank of this transient may be due to absorption of the charge-resonance excited state of TPE. In fact, a weak build-up of the signal at 550 nm is observed, which is absent in the alcoholic solutions. This absorption resembles the weak band at 520 nm in the diphenylmethylradical[35], making it plausible that the charge-resonance form of TPE absorbs here.
This interpretation leads also to the conclusion that the delayed fluorescence[18] of TPE in alkanes around 560 nm must be attributed to emission from the charge-resonance form of TPE. Previously, this emission was assigned to the relaxed S_1 state[17, 19, 20]. The absence of this band in polar liquids is then immediately explained as well. A further consequence of this line of reasoning is that the so-called "prompt" fluorescence[36], peaked near 500 nm, must be due to emission from the relaxed S_1 state, and not from the vertically excited state, as suggested hereto.

Greene[21] suggested in his ps pump-probe study of TPE that transient absorption of the zwitterionic state is located at 420 nm. Pump-probe measurements at the red flank of this band (at 450 nm, dictated by available interference filters) provide no support for this assignment. These data are shown in figure 5.9. Obviously, no dynamics occur other than a slow decay similar to the 500 nm band. Since the absorption is induced instantaneously, and only weakly responds to ethylenic bond twisting, this 420 nm band is assigned to an excitation localized at the phenyl rings. Of course, when excitation pulses of about 30 ps are being used for pump-probe measurements, all dynamics occurring prior to population of the zwitterionic state go unnoticed and this band can perfectly be used as a marker for the lifetime of the zwitterionic state of TPE[22].

5.6 Avoided Crossing and Charge Separation

Now that the states participating in the isomerization process of TPE have been identified, the question arises whether a coherent picture of the isomerization and charge separation dynamics can be generated. A model for this reaction where the avoided crossing between the π-π^* and π^*-π^* potential surfaces plays a crucial role[32] is suggested. Figure 5.10 shows the level scheme that explains all results. After initial relaxation from the Franck-Condon excited state, the system proceeds along the isomerization pathway towards the avoided crossing region. While this is, most likely, a barrierless process for isolated, gas phase TPE molecules, in solvents considerable friction occurs. This phenomenon is taken into account as potential barrier along the twisting coordinate. The energy levels in figure 5.10 thus represent dressed potential energy surfaces.

As discussed in the introduction, near the avoided crossing the surfaces interact strongly by, for instance, a combination of vibronic coupling and solvation dynamics, and new adiabatic states are formed. Landau and Zener have calculated the transition probability for nonadiabatic crossing between two surfaces at an avoided crossing, using a semiclassical description. Their result for the transition probability P_{LZ} between two states that are strongly coupled is[37]:

$$P_{LZ} = \exp\left[-\frac{(\pi\Delta)^2}{h\theta v}\right] \qquad \textbf{(5.10)}$$

where Δ is the smallest gap between the two states, θ is the difference between the slopes of the unperturbed surfaces at the crossing, and v is the classical velocity of the system at the crossing point.

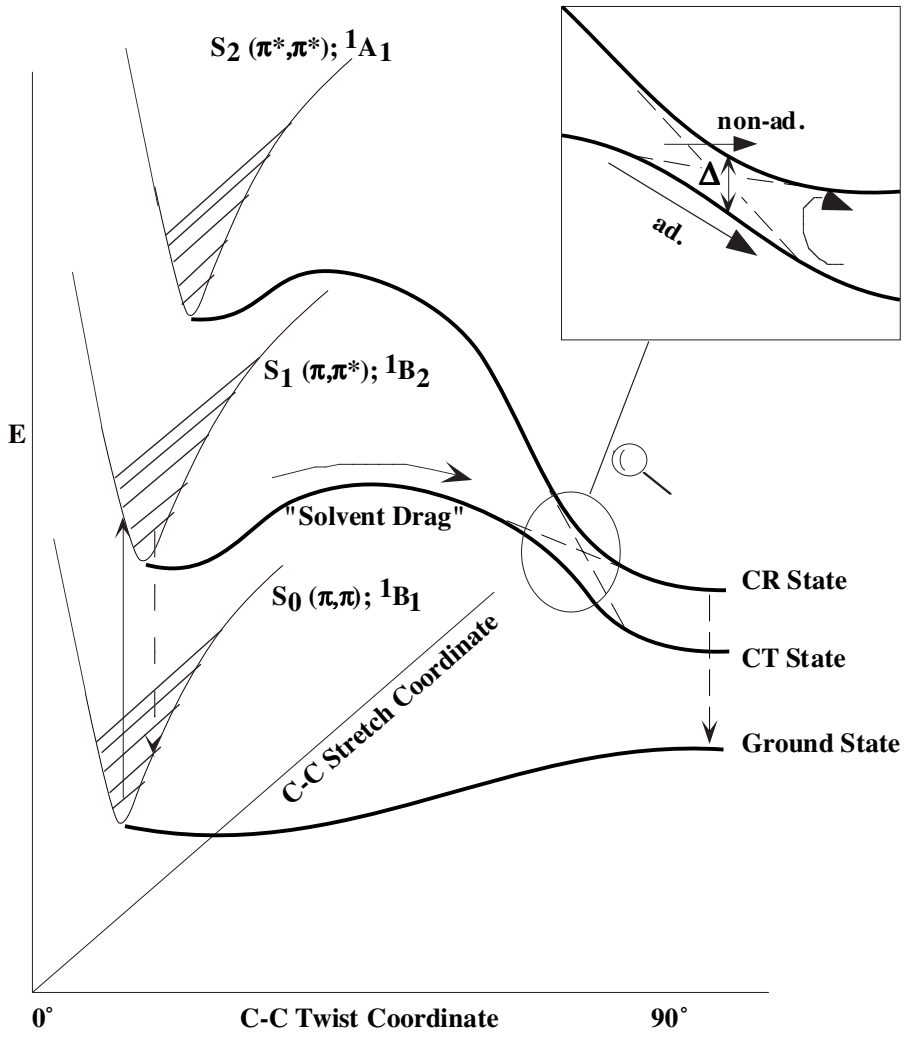

Figure 5.10 Impression of the excited state dynamics of TPE.

It is very difficult to evaluate this expression quantitatively, since the coupling involves dynamic rearrangements of many solvent molecules. In addition, the energy levels themselves depend on the speed of solvent rearrangement when dressed potential energy surfaces are considered. However, it is clear that when the gap at the avoided crossing is large, the reaction proceeds adiabatically to the lower surface. In our case this is the zwitterionic state, carrying a large induced dipole. Nonadiabatic crossing leads to the charge-resonance state, which subsequently relaxes to a state with a minimal induced dipole. The here presented experiments show that in alcohols the zwitterionic state is formed almost exclusively, with only a very small fraction crossing to the upper potential curve. This implies that the charge separation proceeds nearly completely adiabatically through the twisting motion, which is the rate-limiting step in this reaction as well. The

zwitterionic state, thus formed, is stabilized further by solvation. This increases the energy gap with respect to the avoided crossing region so much, that solvent-induced recrossing becomes an improbable event. In addition, radiationless decay to the ground state is a very efficient and competing process. Therefore, in polar solvents the charge-resonance state is not populated by a recrossing process and, consequently, delayed fluorescence from this state is not observed. In nonpolar solvents the reaction proceeds also adiabatically, as can be concluded from the very low efficiency for prompt emission at 560 nm, compared to the steady state quantum yield for this process. However, in this case the zwitterionic state is only stabilized by induced dipoles of the nonpolar solvent, which reduces the gap between the zwitterionic and charge-resonance states such that solvent-induced recrossing to the upper potential is an effective process. Furthermore, radiationless decay to the ground state is slow. Therefore, in nonpolar solvents the charge-resonance state is in thermal equilibrium with the zwitterionic state and delayed fluorescence is observed with a lifetime determined by the lifetime of the zwitterionic state.

This is displayed in figure 5.10, where an impression of the TPE excited state dynamics is given. Subpicosecond relaxation occurs along the C-C stretch coordinate, leading to a large Stokes shift between the excitation wavelength (310 nm, solid arrow), and the probed stimulated emission (500 nm, dashed arrow). The subsequent twist around the central bond is strongly hindered by the surrounding solvent. This is indicated as "solvent drag". The twist leads to adiabatic electron transfer to a zwitterionic state, through an avoided crossing between two excited state potential surfaces. This is designated by ad(iabatic) in the enlarged crossing region of the inset. The resultant charge transfer (CT) state is stabilized by solvent reorganisation. A very small fraction may cross directly to the upper potential curve (non-ad(iabatic) in the inset), which leads to the symmetric charge resonance (CR) state. In nonpolar solvents thermal activation of this nonpolar state is possible, and a dynamic equilibrium between the CT- and CR-states is established.

5.7 Conclusion

From polarization dependent femtosecond pump-probe studies it is concluded that a four state model provides an adequate description for the excited state dynamics of TPE. The four states involved are the Franck-Condon excited state, the relaxed excited state, the charge-resonance state and the zwitterionic state. The sub-picosecond dynamics is attributed to vibrational cooling of the central C-C stretching mode, by strong intramolecular anharmonic mode coupling. The observed 12000 cm^{-1} Stokes shift can be explained by a C-C bond lengthening of about 0.3 Å. The vertically excited state also comprises a wavepacket along the phenyl torsion mode, possibly by coupling to the C-C stretch mode of the ethylenic bond**.** Along the twist coordinate charge-separation occurs near the avoided crossing region in an adiabatic electron-transfer process. Solvent drag limits the speed of twisting, which is the rate limiting step in the reaction. In polar solvents the zwitterionic state, thus formed, is stabilized such that solvent-induced nonadiabatic crossing to the upper potential hardly occurs at all. In nonpolar solvents the energy gap between the two states is less, leading to a thermal equilibrium between the zwitterionic and charge-resonance state. It is this latter state that is responsible for delayed fluorescence.

Crucial in the identification of the various processes is a transient absorption at about 500 nm, which is attributed to the zwitterionic state of TPE. A transient at 450 nm is assigned to a local π-π^* excitation on a $C(Ph)_2$ fragment of the molecule.

5.8 References

1. G. Wald, Science, **162**, 230-239 (1968).
2. Q. Wang, R.W. Schoenlein, L.A. Peteanu, R.A. Mathies and C.V. Shank, Science, **266**, 422-424 (1994).
3. A.A. Heikal, J.S. Baskin, L. Banares and A.H. Zewail, J. Phys. Chem. A, **101**, 572-590 (1997).
4. R.J. Sension, S.T. Repinec, A.Z. Szarka and R.M. Hochstrasser, J. Chem. Phys., **98**, 6291-6315 (1993).
5. A.Z. Szarka, N. Pugliano, D.K. Palit and R.M. Hochstrasser, Chem. Phys. Lett., **240**, 25-30 (1995).
6. T. Ikeda and O. Tsutsumi, Science, **268**, 1873-1875 (1995).
7. N.P.M. Huck, W.F. Jager, B. de Lange and B.L. Feringa, Science, **273**, 1686-1688 (1996).
8. J. Saltiel, J. D'Agostino, D. Megarity, L. Metts, K.R. Neuberger and O.C. Zafiriou, Org. Photochem., **3**, 1-113 (1973).
9. J. Saltiel, J. Am. Chem. Soc., **89**, 1036-1037 (1967).
10. R.J. Buenker, V. Bonacic-Koutecky and L. Pogliani, J. Chem. Phys., **73**, 1836-1849 (1980).
11. R.W.J. Zijlstra, A.H. de Vries and P.Th. van Duijnen, Chem. Phys., **204**, 439-446 (1996).
12. V. Bonacic-Koutecky, P. Bruckmann, P. Hiberty, J. Koutecky, C. Leforestier and L. Salem, Angew. Chem., Int. Ed. Engl., **14**, 575-576 (1975).
13. R.A. McGill, J.K. Rice, A.P. Baranovski, J.C. Owrutsky, A.H. Lowrey, K.K. Stavrev, T. Tamm and M.C. Zerner, Int. J. Quant. Chem. Symp., **30**, 383-394 (1996).
14. K.C. Hasson, F. Gai and P.A. Anfinrud, Proc. Natl. Acad. Sci. U.S.A., **93**, 15124-15129 (1996).
15. A. Stolow, B.A. Balko, E.F. Cromwell, J.-S. Zhang and Y.T. Lee, J. Photochem. Photobiol. A. Chem., **62**, 285-300 (1992).
16. D.B. Toublanc, R.W. Fessenden and A. Hitachi, J. Phys. Chem., **93**, 2893-2896 (1989).
17. W. Schuddeboom, S.A. Jonker, J.M. Warman, M.P. de Haas, M.J.W. Vermeulen, W.F. Jager, B. de Lange, B.L. Feringa and R.W. Fessenden, J. Am. Chem. Soc., **115**, 3286-3290 (1993).
18. J. Morais, J. Ma and M.B. Zimmt, J. Phys. Chem., **95**, 3885-3889 (1991).
19. J. Ma, G. Bhaskar Dutt, D.H. Waldeck and M.B. Zimmt, J. Am. Chem. Soc, **116**, 10619-10629 (1994).
20. P.F. Barbara, S.D. Rand and P.M. Rentzepis, J. Am. Chem. Soc., **103**, 2156-2162 (1981).
21. B.I. Greene, Chem. Phys. Lett., **79**, 51-53 (1981).
22. C.L. Schilling and E.F. Hilinski, J. Am. Chem. Soc., **110**, 2296-2298 (1988).
23. E. Lenderink, K. Duppen and D.A. Wiersma, J. Phys. Chem., **99**, 8972-8977 (1995).
24. E. Lenderink, *Femtosecond Chemistry in Solutions*, Ph.D. thesis, University of Groningen, 1995.

25. R.W.J. Zijlstra, P. Th. van Duijnen, B.L. Feringa, T. Steffen, K. Duppen and D.A. Wiersma, J. Phys. Chem. A, **101**, 9828-9836 (1997).
26. S. Mukamel, *Principles of Nonlinear Optical Spectroscopy*, Oxford University Press, New York, 1995.
27. S. Mukamel, C. Ciordas-Ciurdariu and V. Khidekel, *Time-Frequency and Coordinate-Momentum Wigner Wavepackets in Nonlinear Spectroscopy*, in: Advances in Chemical Physics, Ed: P. Gaspard and I. Burghardt, John Wiley and Sons, Inc., New York, 1997.
28. M.D. Levenson and S.S. Kano, *Introduction to Nonlinear Spectroscopy*, Academic Press, San Diego, 1988.
29. C.J. Bardeen, Q. Wang and C.V. Shank, Phys. Rev. Lett., **75**, 3410-3413 (1995).
30. Y.J. Yan, L.E. Fried and S. Mukamel, J. Phys. Chem., **93**, 8149-8162 (1989).
31. G.R. Fleming, *Chemical Applications of Ultrafast Spectroscopy*, Oxford University Press, New York, 1986.
32. L. Salem, Science, **191**, 822-830 (1976).
33. P. Piotrowiak, G. Strati, J. Warman and W. Schuddeboom, J. Am. Chem. Soc., **118**, 8981-8982 (1996).
34. K. Duppen, F. de Haan, E.T.J. Nibbering and D.W. Wiersma, Phys. Rev. A, **47**, 5120-5137 (1993).
35. A. Bromberg and D.J. Meisel, J. Phys. Chem., 2507-2513 (1985).
36. J. Ma and M.B. Zimmt, J. Am. Chem. Soc., **114**, 9723-9724 (1992).
37. C. Zener, Proc. Roy. Soc. London, A, **137**, 696-702 (1932).